A&A 541, A98 (2012)
DOI: 10.1051/0004-6361/201118389

Astronomy & Astrophysics

Interacting planetary nebulae

I. Classification and orientation⋆

A. Ali[1,2], L. Sabin[3], S. Snaid[1], and H. M. Basurah[1]

[1] Astronomy Dept, Faculty of Science, King Abdulaziz University, Jeddah, Saudi Arabia
e-mail: afmali@kau.edu.sa
[2] Department of Astronomy, Faculty of Science, Cairo University, Egypt
[3] Instituto de Astronomía, Universidad Nacional Autónoma de México, 22800 Ensenada, B.C., Mexico

Received 3 November 2011 / Accepted 15 March 2012

ABSTRACT

We discuss the classification and orientation of planetary nebulae that interact with the interstellar medium throughout the Milky Way. A sample of 117 confirmed interacting planetary nebulae is used for this purpose. Our results indicate that the majority of interacting objects are located close to the Galactic plane, and ∼77% of them are located inside the Galactic thin disk. One third of the sample is less than 100 parsec from the Galactic plane and thus may interact with molecular and cold neutral clouds. There is a tendency for the planetary nebula interaction region to be parallel to the Galactic plane. We found that ∼73% of interacting planetary nebulae have inclination angles (defined as the angles that join the planetary nebula centroid and the interaction area or bow shock with the Galactic plane) larger than 45° and ∼38% larger than 70°, which highlights the possible effect of interstellar magnetic fields. While it is sometime believed that the interaction preferentially occurs in old planetary nebulae, our analysis indicates that the majority of observed planetary nebulae are in the mid stage of their evolution. The mean inclination angle, Galactic height, linear size, and dynamical age are estimated for each stage of interaction. The results indicate strong correlations between the mean inclination angle and the above parameters.

Key words. planetary nebulae: general – methods: statistical

1. Introduction

The interaction between planetary nebulae (PNe) and the interstellar medium (ISM) is an important process whose effects allow us to gain a better understanding of the two components involved. Indeed, on one hand, it is a valuable tool for probing the ISM structure (mainly at small scale) and also for determining some ISM physical properties such as density, filling factor of coronal gas, and magnetic field effect. On the other hand, the PN-ISM interaction phenomenon is helpful for studying the evolution of old PNe and PNe halos. The process can also be used to predict the direction of motion of planetary nebula central stars (CS). Finally, the interaction is an essential key for understanding the "missing mass phenomenon" (i.e. the mass difference between the white dwarf and its parent star) because it traces the return of stellar material into the ISM, which is important for understanding the chemical evolution of the Galaxy.

Theoretical studies on the PN-ISM interaction process started in the late 60s and can be divided into four categories: (1) prediction and simple analytical calculations (Gurzadyan 1969; Smith 1976; Isaacman 1979; Borkowski et al. 1990); (2) numerical simulations (Soker et al. 1991); (3) analytical calculations of instabilities and the role of the interstellar magnetic field (IMF) (Soker & Dgani 1997, hereafter SD97; and Dgani & Soker Dgan98, hereafter DS98); (4) 2D and 3D hydrodynamic simulations (Villaver et al. 2002, 2003; Villaver 2004; Müller et al. 2004; Wareing et al. 2007).

From an observational point of view the detection of interacting planetary nebulae (IPNe) is made difficult by the low surface brightness generally associated with large, evolved and/or diluting nebulae. However, over the years some progress has been made (notably by improving the observing techniques), and in the following we list the most noticeable researches made up to date. Borkowski et al. (1990, hereafter BSS) brought the number of known IPNe to about 17 objects and listed 11 objects as possible IPNe by examining their morphology. CCD imaging campaigns were performed by Xilouris et al. (1996, hereafter X96) and Tweedy & Kwitter (1996, hereafter TK96), who investigated 9 and 19 large aging PNe, respectively. Guerrero et al. (1998) studied 15 multiple shell planetary nebulae whose morphologies strongly indicate an interaction with the ISM, and some other examples of interaction between PNe's halos and the ISM have been shown by Corradi et al. (2003). Kerber and his colleagues combined deep CCD observations of IPN candidates with spectroscopic analysis as a powerful tool to study their physical conditions (Kerber et al. 1998, 2000a, 2002). More recently, Sabin et al. (2010) detected 21 new IPN candidates in the framework of the IPHAS survey, which goes deeper in terms of sensitivity than past surveys and therefore allows us to identify very faint nebulae. Finally, the observation of IPNe was extended to the mid-infrared by Ramos-Larios & Phillips (2009) and Ramos-Larios et al. (2011), who have reported observational evidence for interaction between some PNe halos and the ISM. All these observations are giving us a ground for a larger investigation.

Therefore this paper presents a statistical analysis of a large portion of IPNe known today. It will focus on their physical parameters, their preferential galactic orientation and their morphological classifications according to the criteria defined by Wareing et al. (2007). We established an interacting planetary

⋆ Table 1 is available in electronic form at http://www.aanda.org

nebulae database, which is presented in Sect. 2; the results are discussed in Sect. 3. Our concluding remarks are given in Sect. 4.

2. The database

2.1. The sample

The present sample has been established by collecting IPNe data from a large number of articles discussing the subject. A first selection was made dividing the sample into two groups: confirmed and possible IPNe based on the evidence for interaction. The criteria used to distinguish between both groups are: (1) objects displaying more than one sign of interaction (e.g. flux enhancement and drop of ionization level in the interaction region, filaments due to shock compression by ISM, displacement of central star and asymmetry of the outer region of the nebula) are considered as confirmed IPNe. This concerns most of the objects listed by BSS, TK96, XI96 in addition to those identified as highly reliable IPNe by Soker (1997); (2) objects presented by Ali et al. (2000) as interacting PNe due to their one-sided shape and/or defined by Soker (1997) as low-confidence IPNe and have no other sign of interaction, are considered as possible IPNe. In addition, we can also refer to some other examples for possible IPNe members such as the 21 new IPHAS PN-ISM candidates mentioned earlier (Sabin et al. 2010) and the many other candidates from the "*Macquarie/AAO/Strasbourg*" Hα Planetary Nebula Catalogue – MASH I (Parker et al. 2006) and MASH II (Miszalski et al. 2008). We introduce here the following examples from the MASH catalogs: PN G221.0-01.4, PN G249.8-02.7, PN G238.5+01.7, PN G224.3-03.4, PN G011.2-02.7, PN G315.4-08.4, and PN G307.2-05.4. These objects show a one-sided shape that could be related to an advanced stage of interaction owing to the presence of a bow shock structure.

A caveat, however, is the wrong classification of PNe as IPNe in the literature, either because the objects are simply not true PNe (but mimics, see Frew et al. 2010) or because their morphology does not derive from an ISM interaction process. PHL 932 (HII region, Frew et al. 2010), S181 (HII region, Cazzolato & Pineault 2003), A33 (no sign of interaction, Soker 1990), and Sp3 (wide binary, Soker 1990) are examples of such contaminants.

To better constrain our results we chose to ignore the possible IPNe and focused only on confirmed ones, and therefore 117 objects were selected. In each case, the common PN name, its Galactic coordinate, inclination angle and its associated error, distance, angular radius, linear radius, expansion velocity, Galactic height, dynamical age, and interaction classification of the sample are given in Table 1. The latter is established using the Wareing et al. (WZO in what follows) classification method (Wareing et al. 2007).

2.2. Distances and physical parameters

The accurate determination of the distance of planetary nebulae is necessary to derive essential parameters such as their size, mass, age, luminosity, and Galactic height. It is well known that the individual distances of PNe have better accuracy and are more reliable than statistical distances. Fortunately, roughly half of our sample (62 objects) has known individual distances. These distances are derived from different individual methods such as trigonometric, expansion, extinction, and gravity methods. A mean error on the distance of about 22% is estimated for this group. The mean distance is adopted for objects with more than one measurement.

However, we have to rely on statistical distance estimators for the remaining IPNe. Among the statistical scales is that of Phillips (2002). This scale was derived using the radio surface temperature-radius calibration of 66 nearby nebulae. With this method most of the PNe (radio) flux is then taken into account. Using a statistical scale based on radio fluxes appears to be a safer choice than a scale based on optical flux measurements (for example that using Hα flux, e.g. Frew & Parker 2006) because in our case the rather irregular morphology of the IPNe (particularly the evolved objects) would make the flux and then the distance estimation more difficult to determine accurately. The distances of 39 IPNe in our sample were therefore derived following this method. The mean error on the distance of this group is considered to be 33% (Phillips 2002). Among the objects left, nine PNe have their statistical distances taken from the literature. They are relying on an assumption of a constant physical property such as the ionized mass. This group also has the less accurate distances among our sample (leading to less accurate derived parameters such as the Galactic height). Finally, we were unable to find a distance for seven objects.

The angular radius (θ) and expansion velocity ($V_{\rm exp}$) parameters were also extracted from the literature (e.g. Acker et al. 1992; Weinberger 1989; Pottasch 1996). And for PNe with multiple measurements of expansion velocities, we adopted a mean value. Regarding the objects with unknown $V_{\rm exp}$, we adopted a standard value $V_{\rm exp} = 20$ km s^{-1} (Weinberger 1989). The linear radius (R) and dynamical age ($T_{\rm dyn}$) were subsequently derived and listed in Table 1. Therefore in the latter we find the number, the name, and Galactic coordinates (l, b) of the PNe with the associated references in Cols. 1 to 5, respectively, the measured interaction angle (IA) and its error (e) are given in Cols. 6 and 7, the distances (D) and their measurement methods as well as the associated references are presented in Cols. 8−10, the angular radius (θ) and references are presented in Cols. 11 and 12, and the expansion velocity ($V_{\rm exp}$) and references are given in Cols. 13 and 14. The four last entries are the height above the plane (Z), the radius (R), the dynamical time ($T_{\rm dyn}$), and WZO stage in Cols. 15−18 respectively.

2.3. IPNe orientation

To derive accurate orientation and morphological classification of the sample under investigation, a cautious visual inspection was made involving imaging resources such as The Planetary Nebula Image Catalogue by Bruce Balick[1], the morphological catalog of Northern Galactic Planetary Nebula by Manchado et al. (1996) and the Digitized Sky Survey archives. To deduce the orientation of the interacting (enhanced) region relative to the Galactic plane as simply and accurately as possible, we reproduced each IPN image in a new reference system, i.e., according to their Galactic coordinates using the Sky View Virtual Observatory[2], where the X and Y axes of each image represent the parallel to the Galactic latitude and Galactic longitude, respectively (Fig. 1). The orientation of the enhanced region is determined by measuring its inclination angle (IA), which is ranging from 0° to 90° (Ali et al. 2000). This is defined by the angle between the axis of the interacting rim (defined as a straight line between the PN geometric center and the middle of the PN's enhanced region, which we assume is the direction of propagation

[1] http://www.astro.washington.edu/users/balick/PNIC
[2] http://Skyview.gsfc.nasa.gov

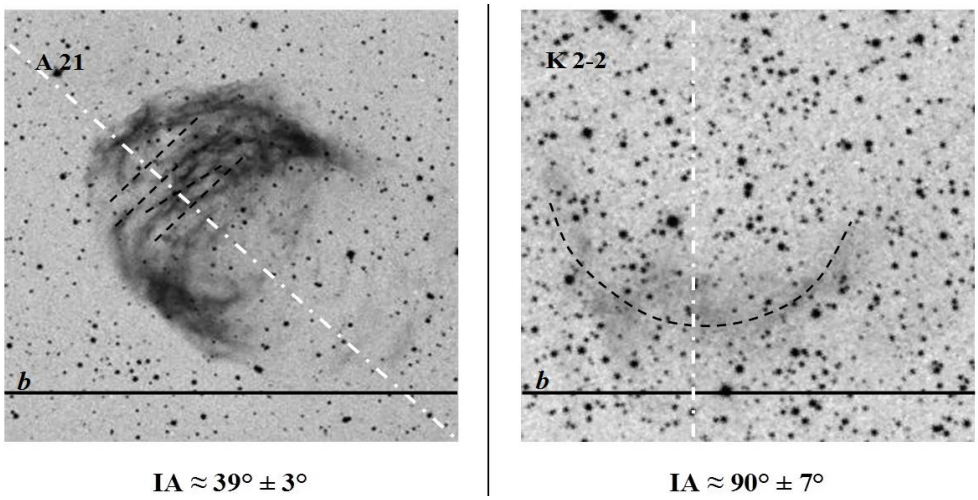

Fig. 1. Two examples showing the measurement method of the inclination angle. A21 on the left, which displays stripes inside its main body and K2-2 on the right, showing a semi-circular bow-shock. The straight or curved black dashed line represents the interaction area, the white dot-dashed line represents the axis of interaction and the black solid line represents the axis parallel to Galactic plane. Both images are from the Digitized Sky Survey.

of the bow shock into the interstellar material and is represented by a white dot-dashed line in Fig. 1) and the axis parallel to the Galactic plane (represented by a black solid line in Fig. 1). When the two axes are perpendicular to each other (IA = 90°), the interaction area is parallel to the Galactic plane (see for example the case of IPN K2-2 in Fig. 1). Also, when the IA ∼ 75°, the enhanced region will have only ∼15° margin before being fully parallel to the Galactic plane, and so on. A source of error in the measurement of the inclination angle is based on the quality of the image. When the interaction area is well-defined, the uncertainty will not exceed ±2°.

A similar work was compiled by Ali et al. (2000), and they showed that of an overall sample of 40 one-sided PNe, a third display an orientation roughly parallel to the Galactic plane.

3. Results and discussion

3.1. Galactic distribution of the sample

Generally, the galactic distribution of the sample (Fig. 2) does not show any preferential location for the occurrence of interaction between PNe and the ISM. However, we can point out that the majority of the objects are located close to the Galactic plane with a mean absolute Galactic latitude $\langle|b|\rangle = 12°$ (Table 2).

Figure 3 shows the distribution of IPNe according to their Galactic height. The associated error is mainly caused by the error on the distance. An estimated error range $\sigma(\Delta z)$ of 22−42% was derived for the distribution.

Figure 3 and Table 1 also reveal that around 77% of the sample is located within the thin Galactic disk ($z < 400$ pc, X96)[3]. Therefore, they are coexisting with the molecular, cold neutral and warm neutral interstellar media. The patchy nature of these media and the (sometime) large Galactic height range make any strong claim on the exact location of the IPNe difficult. However, we observe that roughly one-third of the sample shares the same area as molecular clouds ($z \leq 75$ pc, Spitzer 1978) and cold neutral medium ($z \leq 100$ pc, Heiles & Troland 2003).

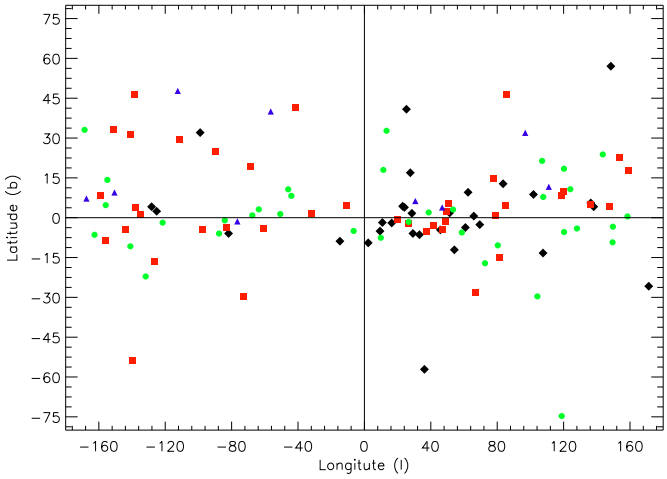

Fig. 2. Galactic distribution of the IPNe sample according to the WZO stages defined by Wareing et al. (2007): black diamond: WZO1, red square: WZO2, green circle: WZO3 and blue triangle: WZO4.

This dense part of our galaxy makes the PNe-ISM interaction very probable and more noticeable in both media. The density number of the molecular medium is larger than 10^3 cm^{-3} and its temperature is ∼20 K, while the cold neutral medium has a density range from 20 to 60 cm^{-3} and a temperature of ∼100 K (Dopita & Sutherland 2003). Our result here gives higher probability for detecting IPNe toward the molecular and cold media, in contrast to BSS, who expected few interacting PNe because of the low filling factor of those environments.

Planetary nebulae moving with low or moderate velocity through high-density media (e.g. HFG1 located at $z \sim 40$ pc with relative velocity ∼40 km s^{-1}, Ali et al., in prep.) are expected to create isothermal shocks as they interact with the ISM. In this case the cooling time post shock becomes shorter than

[3] The peculiar radial velocity ($|\Delta V|$, the difference between the observed local standard of rest radial velocity, and the velocity determined from the rotation curve) was calculated for the objects with available radial velocity data. We found that $\langle|\Delta V|\rangle \sim 36$ km s^{-1} for IPNe with $z \leq 400$ pc (45 objects) and $\langle|\Delta V|\rangle \sim 71$ km s^{-1} for IPNe with $z \geq 400$ (12 objects). Quireza et al. (2007) and Maciel & Dutra (1992) show that objects belonging to the Galactic thin disk should have $|\Delta V| \leq 60$ km s^{-1}. Therefore this result, which is applicable to half of our sample, can be used as another argument to show that the majority of IPNe with $z \leq 400$ pc are indeed consistent with the Galactic thin disk.

Table 2. Characteristics of the four different stages of interaction.

WZO stage	$\langle\|b\|\rangle$	$\langle\|Z\|\rangle$ (pc)	$\langle R\rangle$ (pc)	$\langle T_{\rm dyn}\rangle$ (yrs)	$\langle$IA$\rangle$
WZO1	12.0°(31)	274(30)	0.17(30)	08.5E+03(30)	54.0 ± 7.9(28)
WZO2	14.3°(40)	362(38)	0.48(38)	21.2E+03(38)	56.3 ± 7.1(39)
WZO3	11.7°(36)	190(31)	0.64(31)	40.2E+03(31)	61.4 ± 9.1(36)
WZO4	17.7°(09)	115(08)	0.83(08)	67.6E+03(08)	76.6 ± 11.0(09)
Weighted Mean	12.0°(116)	269(107)	0.47(107)	26.6 E+03(107)	59.0 ± 8.3(112)

Table 3. Consistency of the three IPNe classifications.

Wareing et al. (2007)	Features	Rauch et al. (2000)	TK96
WZO1	Halo interaction	young	H
WZO2	Spherical PN with enhanced brightness in the interaction region.	mid-age	B, S or F
WZO3	Displacement of the CS; One-sided PNe and instabilities.	old	C
WZO4	The CS stripped outside the PN.	old	–

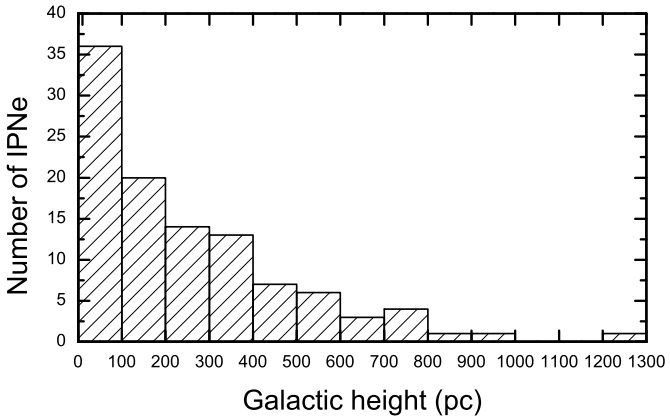

Fig. 3. Number of IPNe according to their Galactic heights above the plane.

the flow time and the magnetic pressure overcomes the thermal pressure (SD97). Around 55% of our sample exists at $z \leq 200$ pc. Figure 3 shows that ~23% of the sample is located within the Galactic thick disk and Galactic halo. The chance of interactions of these objects is low. The high-velocity PNe moving through these low-density media (e.g. NGC 7094 located at $z \sim 800$ pc with relative velocity of ~200 km s^{-1}, Ali et al., in prep.) are expected to undergo adiabatic shocks when the cooling time post shock becomes longer than the flow time and the thermal pressure overcomes the magnetic pressure (SD97).

We derived a mean absolute Galactic height $\langle|z|\rangle = 270$ pc for our sample (Table 2), although we point out the uncertainty on the statistical distances of some objects. About 62% of the sample has a mean absolute latitude $\langle|b|\rangle$ below 10° with a mean value of 4.5° and a mean absolute Galactic height of 151 pc, and the remaining 38% has $\langle|b|\rangle$ above 10° with a mean value of 27.2° and a mean absolute Galactic height of 468 pc. Sn1 and JaFu2, which are globular cluster members, were not considered while deriving the mean values of b, z, and consequently the other parameters.

3.2. The interacting nebulae classifications

Three different classifications were established for the PNe-ISM interaction process. TK96 introduced a short code describing the IPNe morphologies: B (bipolar PNe); F (uniformly filled); H (halo-interaction); S (thick shell) and C (crescent-shaped). Based on the age and strength of interaction, Rauch et al. (2000) characterized three different stages of interaction: young, middle-aged, and old. Wareing et al. (2007) introduced four evolutionary stages for IPNe through their triple-wind model. Hence during their WZO1 stage the PN is not affected and a faint bow shock may be observable due to the interaction between the AGB wind and the ISM (as discussed by Villaver et al. 2003). The WZO2 stage is characterized by a brightening of the PN shell in the direction of motion. During the WZO3 phase the central star shifts away from the geometric center and ultimately the PN appears completely disrupted with its central star located outside the PN in the so-called WZO4 stage. The classifications of TK96 and Rauch et al. (2000) are generally consistent with that of Wareing et al. (2007) as illustrated in Table 3.

In the present analysis, we chose to work with the scheme by Wareing et al. (2007). The results are presented in the final column of Table 1 and the average parameters derived for each stage are presented in Table 2. Hence, the mean absolute Galactic latitude $\langle|b|\rangle$ does not seem to vary noticeably from one stage to another, although we can still point out that WZO4 IPNe seem to be located at higher latitudes on average than the rest of the sample.

Table 2 also reveals that the majority of IPNe are observed in association with the WZO2 and WZO3 stages, while the least observed members are associated with WZO4 stage. This result should be handled with care as it could reflect a detection bias rather than a real pattern. Indeed, the relatively low surface brightness associated with WZO4 IPNe combined with the high interstellar extinction close to Galactic plane, where the majority of these objects are located (see below), make them difficult to identify/detect (therefore surveys such as IPHAS and MASH are expected to contribute to solving this problem). In contrast, WZO2 and WZO3 IPNe are more likely to be detected via their bright rim.

In terms of evolutionary status, the results show that there is an obvious trend of increasing dynamical time ($T_{\rm dyn}$) with the interaction evolution stages, which was to be expected. The earliest stage of interaction occurs at $T_{\rm dyn} \sim 8500$ years, while the most advanced stage occurs at $T_{\rm dyn} \sim 67\,600$ years (Table 2). During the PN evolution, its size and ionized mass increase whilst its density decreases, especially after the PN passes the transition between the optically thick and the optically thin limit. So, we expect a strong correlation between the size and age

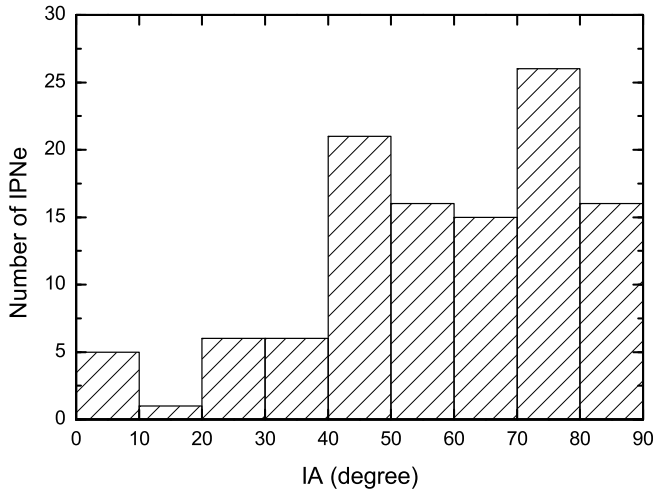

Fig. 4. Distribution of the measured inclination angles of the sample.

of PNe. Our results given in Table 2 indeed confirm this trend (with a correlation factor $r = 0.96$) between R and $T_{\rm dyn}$ where the radius increases from WZO1 to WZO4 stage. In calculating the average radius of the WZO4 stage, we ignored the peculiar PG 1034+001 nebula that represents the largest known interacting nebula and has a radius ~8 pc. The mean radius of the sample is on average five times the standard value of $\langle R\rangle = 0.1$ pc (Pottasch 1983). This would indicate that most of the IPNe in the sample are in their middle and advanced stage of evolution.

We also calculated the mean absolute height $\langle|z|\rangle$ for each stage. The WZO2 stage shows the highest value, followed by the WZO1, WZO3, and finally the WZO4 stage, respectively, closer to the Galactic plane. There is a trend of decreasing $\langle|z|\rangle$ with the advancement of interaction stages and consequently with PN age, except for WZO2. The correlation between $\langle|z|\rangle$ and $\langle T_{\rm dyn}\rangle$ shows an inverse relation with a coefficient $r = -0.85$ (Table 2). The two evolutionary younger stages of interaction tend to exist at higher Galactic height compared with the other two more advanced stages.

3.3. The Galactic orientation of IPNe

Studying the orientation of planetary nebulae is very common (e.g. Shain 1956; Grinin & Zvereva 1968; Akhundova & Seidov 1970; Melnick & Harwit 1975; Phillips 1997; Corradi et al. 1998; Weidmann & Díaz 2008). It provides information about mechanisms capable of explaining the various shapes of PNe such as bipolar and elliptical objects. For IPNe, Ali et al. (2000) investigated the spatial orientation and distribution of one-sided PNe. This time we investigate the orientation of IPNe with respect to the Milky Way based on a larger sample.

We successfully measured the inclination angle (IA, as defined before) for 112 objects in our sample (Table 1). We found that while ~73% of the sample has IA > 45°, ~38% has IA > 70° (Fig. 4). This result is consistent with that achieved by Ali et al. (2000), regardless of the differences between the two samples. Figure 4 shows the increase of IPNe frequency with the inclination angle.

The reason for this orientation is still under debate. Soker & Zucker (1997) suggested that the gas responsible for the long stripes in the outer region surrounding NGC 6894 has been ionized by its central star and could originate from the stripping of the object's halo by the ISM. They speculate that the stripes were shaped by the interstellar magnetic field (IMF) due to their orientation, which coincides with that of the IMF lines in the Galaxy (Mathewson & Ford 1970). Disregarding the particular problem raised by the stripes' origin (*see below*) and following Soker & Zucker (1997) on the correlation IMF/IPNe orientation for the total sample, our results deduced from Fig. 4 indicate that more than one-third of the sample (42 objects) has a direction of interaction roughly parallel to the Galactic plane with an orientation within 20° of it, so the interstellar magnetic field might play an important role in shaping the interacting regions of these PNe.

The only direct observational evidence for the role of IMF in shaping IPNe was given by Ransom et al. (2008). Using the estimate of the rotation measure and the electron density in the shell of S216 nebula, they derived a line-of-sight magnetic field in the interaction region of $5.0 \pm 2.0\,\mu$G. Very recently, Ransom et al. (2010) showed the influence of the IMF in the interacting DHW5 by studying the Faraday rotation structure in the inner tail of the object. This particular subject will be discussed in a forthcoming article.

Except for the IMF, few other mechanisms can explain the alignment with respect to the Galactic plane. Phillips (1997) quoted some of them to interpret the orientation of a sample of binary PNe parallel to the plane. Therefore the preferential orientation of binary systems, the orientation of the angular momentum vectors of molecular clouds parallel to the plane, or the temporal orientation of the axis of mass-loss ejection have been suggested. Unfortunately, none of these hypotheses, which could be applied to the IPNe, is supported by strong observational evidence. We also looked for kinematical studies that would give an indication on a possible preferential orientation on the dynamical motions of IPNe or even PNe (without "any" marked ISM interaction), i.e., indicating a strong velocity component perpendicular to the Galactic plane, but we found no exhaustive investigation. However, the recently released *San Pedro Mártir Kinematic Catalogue of Galactic Planetary Nebulae* (López et al. 2012), which contains detailed kinematical information of hundreds of PNe including IPNe, is likely to provide an answer to the role of kinematics in the alignment with the Galactic plane in the near future.

Finally, our results in Table 2 also show a strong correlation between the mean inclination angle $\langle$IA$\rangle$ and $\langle|z|\rangle$, $\langle R\rangle$ and $\langle T_{\rm dyn}\rangle$. The correlation coefficient between $\langle$IA$\rangle$ and $\langle|z|\rangle$ is -0.87. This indicates that the interaction tends to be parallel for objects close to the plane, and this tendency becomes less noticeable as we move away from it.

3.4. Striped PNe

Striped planetary nebulae are believed to provide observational evidence of the effect of the IMF in shaping IPNe. Indeed, Dgani & Soker (1998) stated that RT instability can fragment the halo of PNe and thereby allow the ISM to flow into their inner regions. They presented four criteria to define the striped PNe, and illustrated the different morphologies in their Fig. 3. However, the study of striped PNe and their relation with the IMF is hampered by the large uncertainties on the origin of the stripes themselves. Indeed, few kinematical investigations on those particular objects and at those particular locations have been realized. They would indicate a difference or an agreement in radial velocity between the stripes and the main nebula, which would lead to a different or common origin, respectively (e.g. the case of NGC 6751 where the most outer stripes in the northeast turned out to be an ISM pattern (Chu et al. 1991; and Clark et al. 2010). The size, height, inclination angle, and WZO classification of 19 striped PNe are listed in Table 4. In this list only two

Table 4. List and properties of striped PNe in our sample.

No.	PN	l	b	IA	e	Z (pc)	R (pc)	T_{dyn} (yrs)	WZO stage
1	A 21	205.14	14.24	39	3	138	0.83	1.81E+04	WZO3
2	A 35	303.57	40.00	78	3	117	0.31	7.51E+04	WZO4
3	DHW 5	111.09	11.64	84	12	67	0.42	8.27E+04	WZO4
4	EGB 9	209.43	9.50	83	5	57	0.25	1.24E+04	WZO4
5	HDW 5	218.99	–10.78	72	19	369	0.45	2.19E+04	WZO3
6	HW 4	149.50	–9.28	90	8	62	0.50	2.44E+04	WZO3
7	IW 2	107.73	7.81	43	13	89	1.42	1.16E+05	WZO3
8	NGC 3242	261.05	32.05	76	13	235	0.03	1.11E+03	WZO1
9	NGC 40	120.02	9.87	90	3	138	0.09	3.46E+03	WZO2
10	NGC 6894*	69.48	–2.62	90	11	46	0.10	2.21E+03	WZO1
11	PW 1	158.92	17.86	76	8	104	0.97	3.84E+04	WZO2
12	RE 1738+665	96.89	31.96	76	13	106	1.66	8.12E+04	WZO4
13	S 176	120.29	–5.40	82	4	59	1.10	5.67E+04	WZO3
14	S 188	128.05	–4.07	47	8	46	0.54	1.31E+04	WZO3
15	S 200	138.13	4.12	25	9	42	0.48	3.60E+04	WZO1
16	S 216	158.49	0.47	62	5	1	1.89	2.64E+05	WZO3
17	SuWt 1	309.30	1.39	87	12	13	0.09	4.25E+03	WZO3
18	Ton 320	191.40	33.08	39	6	202	1.53	7.48E+04	WZO3
19	YM 16	38.71	1.97	56	6	17	0.37	1.80E+04	WZO3

Notes. The table shows the number and name of the PNe (1, 2), the Galactic longitude and latitude (3, 4), the interaction angle and associated error (5, 6) and finally the height above the plane, the radius, the dynamical time and interaction stage (7−10). (*) Possible striped PN (see text).

PNe have kinematics data related to their stripes: NGC 3242 (Meaburn et al. 2000), where the link between the filamentary system and the main PN is still unclear, and the well-studied Sh 2-188 (Rosado & Kwitter 1982; and Wareing et al. 2006), where the stripes are indeed related to the PN. However, and to quote Soker & Zucker (1997) in their analysis of the stripes in NGC 6894 and their relation with the IMF, it would be a "fortuitous coincidence" for all the structures to be located only at those particular location, at "ionization range" of those 19 IPNe and to have unrelated origins (e.g. ISM filaments). This is even more remarkable for IPNe showing curved stripes and a thin morphology. If we assume this, the mean inclination angle of the interaction areas ($\langle IA \rangle \simeq 70° \pm 8°$) indicates that the striped PNe are mainly parallel to the Galactic plane. Based on their adopted distances we localize all of them in the thin Galactic disk, where the mean vertical height from the Galactic plane is about 100 pc. We also note that the small IA of some objects such as Ton 320 and A21, which are located at high latitudes, could reflect the local orientation of IMF lines in those areas where more precise observations are needed. The lack of kinematical information is a strong handicap and the kinematic catalog by López et al. (2012) would here again be a valuable tool to help solving this long-standing problem.

4. Conclusions

We discussed the classification and orientation of a large sample of IPNe. Overall, the results show that the majority of interaction regions are parallel to the Galactic plane and appear to be strongly correlated to the direction of the IMF lines. The effect of the IMF in shaping the interaction area is highlighted, although we do not discard the role and influence of other dynamical motions such as IPNe kinematics. We observed a similar pattern after studying 19 striped PNe, which would need deeper kinematic investigation to ascertain the link between the stripes and the main nebula. The main results of our statistical analysis are summarized as follows: (1) the distribution of IPNe shows non-preferential locations for interaction in the Milky Way, except for a concentration close to the Galactic plane; (2) the majority of IPNe are moving through the thin disk and have a high probability to follow isothermal shocks and be subject to magnetic pressure; (3) the number of IPNe coexisting with the molecular and cold neutral media are larger than previously expected in the literature; (4) the majority of the interaction regions have a tendency to be parallel to the Galactic plane, especially for the objects very low on the plane, which are in a more advanced stage of interaction; (5) the interaction is more likely observable in the mid stages of interaction, WZO2 and WZO3, rather than the early and advanced stages of interaction, WZO1 and WZO4; (6) the IPNe frequency tends to increase with the inclination angle (the majority of the IPNe having large IA) and IPNe frequency tends to decrease with the Galactic height (few IPNe are found at high latitudes).

Acknowledgements. It is a great pleasure for the authors to express their gratitude to the Deanship of Scientific Research at King Abdulaziz University, where this work has been carried out as a part of sponsored researches project (Project No: 3-75/430). L.S. is supported by PAPIIT-UNAM grant IN109509 (Mexico). The authors thank the referee W. Steffen for his valuable comments, which improved the paper. We are indebted to H. A. Ismail for fruitful discussions and help. This research has made use of the SkyView developed by NASA under the auspices of the HEASARC at the NASA/GSFC Astrophysics Science Division.

References

Acker, A., Ochsenbein, F., Stenholm, B., et al. 1992, Strasbourg ESO catalog of Galactic Planetary Nebulae (ESO publications)
Acker, A., Fresneau, A., Pottasch, S. R., et al. 1998, A&A, 337, 253
Akhundova, G. V., & Seidov, Z. F. 1970, SvA, 14, 104
Ali, A. 2006, Bull. Faculty Sci., 75(A), 47
Ali, A., & Basurah, H. M. 2008, King Abdul Aziz University sponsored researches projects, Project No.: 427/178
Ali, A., & Pfleiderer, J. 1999, A&A, 351, 1036
Ali, A., El-Nawawy, M. S., & Pfleiderer, J. 2000, Ap&SS, 271, 245
Aryal, B., Rajbahak, C., & Weinberger, R. 2009, Ap&SS, 323, 323
Benedict, G. F., McArthur, B. E., Napiwotzki, R., et al. 2009, AJ, 138, 1969
Bensby, T., & Lundstrom, I. 2001, A&A, 374, 599
Bond, H. E., & Livio, M. 1990, ApJ, 355, 568
Borkowski, K. J. 1993, IAUS, 155, 307
Borkowski, K. J., Sarazin, C. L., & Soker, N. 1990, AJ, 360, 173 (BSS)
Cahn, J. H., & Kaler, J. B. 1971, ApJS, 22, 319

Cazetta, J. O., & Maciel, W. J. 2001, Ap&SS, 277, 393
Cazzolato, F., & Pineault, S. 2003, AJ, 125, 2050
Chu, Y.-H., Manchado, A., Jacoby, G. H., et al. 1991, ApJ, 376, 150
Clark, D. M., García-Díaz, Ma. T., López, J. A., et al. 2010, ApJ, 722, 1260
Corradi, R. L. M., & Schwarz, H. E. 1995, A&A, 293, 871
Corradi, R. L. M., Aznar, R., & Mampaso, A. 1998, MNRAS, 297, 617
Corradi, R. L. M., Schönberner, D., Steffen, M., & Perinotto, M. 2003, MNRAS, 340, 417
Cudworth, K. M. 1990, AJ, 99, 1863
Cudworth, K., & Peterson, R. C. 1988, IAUS, 126, 523
Dengel, J., Hartl, H., & Weinberger, R. 1980, A&A, 85, 356
Dgani, R., & Soker, N. 1998, ApJ, 495, 337
Dopita, M. A., & Sutherland, R. S. 2003, Astrophysics of the diffuse universe (Berlin, New York: Springer)
Frew, D. J., & Parker, Q. A. 2006, IAU Symp. 234, ed. M. J. Barlow, & R. H. Mendez (Cambridge University Press), 49
Frew, D. J., Madsen, G. J., O'Toole, S. J., & Parker, Q. A. 2010, PASA, 27, 203
Frew, D. J., Stanger, J., Fitzgerald, M., et al. 2011, PASP, 28, 83
Gathier, R., Pottasch, S. R., & Goss, W. M. 1986, A&A, 157, 191
Giammanco, C., Sale, S. E., Corradi, R. L. M., et al. 2011, A&A, 525, A58
Grinin, V. P., & Zvereva, A. M. 1968, Ap, 4, 43
Guerrero, M. A., Villaver, E., & Manchado, A. 1998, ApJ, 507, 889
Guerrero, M. A., Chu, Y.-H., Manchado, A., et al. 2003, AJ, 125, 3213
Gurzadyan, G. A. 1969, Planetary Nebulae (New York: Gordon & Breach)
Harris, H. C., Dahn, C. C., Canzian, B., et al. 2007, AJ, 133, 631
Hartl, H., & Weinberger, R. 1987, A&AS, 69, 519
Heiles, C., & Troland, T. H. 2003, ApJ, 586, 1067
Hippelein, H., & Weinberger, R. 1990, A&A, 232, 129
Isaacman, R. 1979, A&A, 77, 327
Ishida, K., & Weinberger, R. 1987, A&A, 178, 227
Jacoby, G. H. 1981, AJ, 244, 903
Jacoby, G. H., & Van de Steene, G. 1995, AJ, 110, 1285
Jacoby, G. H., Morse, J. A., Fullton, L. K., et al. 1997, AJ, 114, 2611
Kaler, J. B., & Feibelman, W. A. 1985, ApJ, 282, 719
Kaler, J. B., Mo, J.-E., & Pottasch, S. R. 1985, ApJ, 288, 305
Kerber, F. 1998, RvMA, 11, 161
Kerber, F., Groebner, H., Lercher, G., et al. 1997, A&A, 324, 1149
Kerber, F., Roth, M., Manchado, A., et al. 1998, A&AS, 130, 501
Kerber, F., Furlan, E., Rauch, T., et al. 2000a, ASPC, 199, 313
Kerber, F., Furlan, E., Roth, M., et al. 2000b, PASP, 112, 542
Kerber, F., Guglielmetti, F., Mignani, R., et al. 2002, A&A, 381, L9
Kohoutek, L. 1962, BAICz, 13, 120
Kwitter, K. B., Lydon, T. J., & Jacoby, G. H. 1988, AJ, 96, 997
Lopez, J. A., Richer, M. G., Garcia-Diaz, M. T., et al. 2012, RMA&A, 48, 3
Maciel, W. J., & Dutra, C. M. 1992, A&A, 262, 271
Manchado, A., Guerrero, M. A., Stanghellini, L., et al. 1996, The IAC Morphological Catalog of Northern Galactic planetary nebulae
Martin, J., Xilouris, K., & Soker, N. 2002, A&A, 391, 689
Mathewson, D. S., & Ford, V. L. 1970, ApJ, 160, L43
Meaburn, J., Clayton, C. A., Bryce, M., et al. 1998, MNRAS, 294, 201
Meaburn, J., López, J. A., & Noriega-Crespo, A. 2000, ApJS, 128, 321
Mellema, G. 2004, A&A, 416, 623
Melmer, D., & Weinberger, R. 1990, MNRAS, 243, 236
Melnick, G., & Harwit, M. 1975, MNRAS, 171, 441
Miszalski, B., Parker, Q. A., Acker, A., et al. 2008, MNRAS, 384, 525
Müller, H. R., Kerber, F., Rauch, T., et al. 2004, ASPC, 313, 292
Muthu, C., Anandarao, B. G., & Pottasch, S. R. 2000, A&A, 355, 1098
Napiwotzki, R. 1999, A&A, 350, 101
Napiwotzki, R. 2001, A&A, 367, 973
Napiwotzki, R., & Schonberner, D. 1995, A&A, 301, 545
Parker, Q. A., Acker, A., Frew, D. J., et al. 2006, MNRAS, 373, 79
Pierce, M. J., Frew, D. J., Parker, Q. A., et al. 2004, PASA, 21, 334
Phillips, J. P. 1984, A&A, 137, 92
Phillips, J. P. 1997, A&A, 325, 755
Phillips, J. P. 2002, ApJS, 139, 199
Pottasch, S. R. 1980, A&A, 89, 336
Pottasch, S. R. 1983, IAUS, 103, 391
Pottasch, S. R. 1996, A&A, 307, 578
Pottasch, S. R., & Acker, A. 1998, A&A, 329, L5
Quireza, C., Rocha-Pinto, H. J., & Maciel, W. J. 2007, A&A, 475, 217
Ramos-Larios, G., & Phillips, J. P. 2009, MNRAS, 400, 575
Ramos-Larios, G., Phillips, J. P., & Cuesta, L. C. 2011, MNRAS, 411, 1245
Ransom, R. R., Uyaniker, B., Kothes, R., & Landecker, T. L. 2008, ApJ, 684, 1009
Ransom, R. R., Kothes, R., Wolleben, M., & Landecker, T. L. 2010, ApJ, 724, 946
Rauch, T. 1999, A&AS, 135, 487
Rauch, T., & Kerber, F. 2005, ASP Conf. Ser. 334, ed. D. Koester, & S. Moehler (San Francisco: ASP), 329
Rauch, T., Köppen, J., Napiwotzki, R., et al. 1996, A&A, 347, 169
Rauch, T., Furlan, E., Kerber, F., et al. 2000, ASPC, 199, 341
Rauch, T., Kerber, F., & Pauli, E.-M. 2004, A&A, 417, 647
Rodríguez, M., Corradi, R. L. M., & Mampaso, A. 2001, A&A, 377, 1042
Rosado, M., & Kwitter, K. B. 1982, RMA&A, 5, 217
Sabbadin, F. 1984, A&AS, 58, 273
Sabbadin, F. 1986, A&AS, 64, 579
Sabin, L., Zijlstra, A. A., Wareing, C. J., et al. 2010, PASA, 27, 166
Saurer, W. 1995, A&A, 297, 261
Shain, G. A. 1956, SvA, 1, 1
Smith, H. 1976, MNRAS, 175, 419
Soker, N. 1990, AJ, 99, 1869
Soker, N. 1997, ApJS, 112, 487
Soker, N. 1999, AJ, 118, 2424
Soker, N., & Dgani, R. 1997, ApJ, 484, 277
Soker, N., & Hadar, R. 2002, MNRAS, 331, 731
Soker, N., & Zucker, D. 1997, MNRAS, 289, 665
Soker, N., Borkowski, K. J., & Sarazin, C. L. 1991, AJ, 102, 1381
Spitzer, L. Jr. 1978, JRASC, 72, 349
Tajitsu, A., & Tamura, S. 1998, AJ, 115, 1989
Tweedy, R. W., & Kwitter, K. B. 1994a, AJ, 108, 188
Tweedy, R. W., & Kwitter, K. B. 1994b, ApJ, 433, L93
Tweedy, R. W., & Kwitter, K. B. 1996, ApJS, 107, 255 (TK96)
Tweedy, R. W., & Napiwotzki, R. 1994, AJ, 108, 978
Tweedy, R. W., Martos, M. A., & Noriega-Crespo, A. 1995, ApJ, 447, 257
Vauclair, G., Moskalik, P., Pfeiffer, B., et al. 1998, Baltic Astron., 7, 99
Villaver, E. 2004, ASPC, 313, 426
Villaver, E., Manchado, A., & García-Segura, G. 2002, ApJ, 581, 1204
Villaver, E., García-Segura, G., & Manchado, A. 2003, ApJ, 585, L49
Wareing, C. J. 2010, PASA, 27, 220
Wareing, C. J.,O'Brien, T. J., Zijlstra, A. A., et al. 2006, MNRAS, 366, 387
Wareing, C. J., Zijlstra, A. A., & O'Brien, T. J. 2007, MNRAS, 382, 1233
Weidmann, W. A., & Díaz, R. 2008, PASP, 120, 380
Weinberger, R. 1989, A&AS, 78, 301
Weinberger, R., & Aryal, B. 2004, ASPC, 313, 112
Weinberger, R., & Sabbadin, F. 1981, A&A, 100, 66
Werner, K., Heber, U., & Hunger, K. 1991, A&A, 244, 437
Xilouris, K. M., Papamastorakis, J., Paleologou, E., et al. 1996, A&A, 310, 603 (X96)
Zhang, C. Y. 1993, ApJ, 410, 239

Pages 8 to 10 are available in the electronic edition of the journal at http://www.aanda.org

Table 1. The main parameters of the interacting planetary nebulae sample.

No.	PN	l	b	Ref.	IA	e	D (pc)	Method	Ref.	θ ($''$)	Ref.	$V_{\rm exp}$ (km s^{-1})	Ref.	Z (pc)	R (pc)	$T_{\rm dyn}$ (yrs)	WZO stage
1	A 13	204.02	–8.52	1, 2	57	8	944	Ph02		76.5	1	21.3	1	140	0.35	1.61E+04	WZO2
2	A 15	233.53	–16.31	1	70	4	1460	Ph02		17	1	35	1	416	0.12	3.37E+03	WZO2
3	A 16	153.77	22.83	1, 2	55	5	1912	Ph02		52.5	1	20		762	0.49	2.38E+04	WZO2
4	A 19	200.79	8.45	1	78	8	2609	Ph02		33.5	1	20		385	0.42	2.07E+04	WZO2
5	A 21	205.14	14.24	3, 4, 5, 6	39	3	557	Ind	1, 2	307.5	1	45	2	138	0.83	1.81E+04	WZO3
6	A 30	208.56	33.29	7			1155	Ind	9, 10	63.5	1	40	1	671	0.36	8.70E+03	WZO2
7	A 31	219.13	31.29	4, 5, 9	41	4	779	Ind	2, 12	485	1	22.5	1	425	1.83	7.97E+04	WZO2
8	A 34	248.71	29.54	9	80	9	773	Ph02		145	1	34	1	399	0.54	1.57E+04	WZO2
9	A 35	303.57	40.00	4, 5, 6, 11	78	3	167	Ind	1, 4	385	1	4.07	1	117	0.31	7.51E+04	WZO4
10	A 36	318.46	41.50	1, 4	85	8	370	Ind	1, 3	185	1	35	1	268	0.33	9.28E+03	WZO2
11	A 45	20.20	–0.65	5	60	11	700	St	17	142.5	1	20		8	0.48	2.37E+04	WZO2
12	A 52	50.41	5.29	1, 2, 3	28	5	3407	Ph02		18.5	1	20		314	0.31	1.50E+04	WZO2
13	A 58	37.60	–5.16	1, 2, 6	75	8	4807	Ph02		20	1	20		433	0.47	2.28E+04	WZO2
14	A 59	53.40	3.06	2, 12	72	16	1247	Ph02		43.5	1	20		67	0.26	1.29E+04	WZO3
15	A 6	136.10	4.93	1	45	5	1203	Ph02		93	1	20		104	0.54	2.65E+04	WZO2
16	A 61	77.70	14.78	9	90	6	1380	Ind	12	100	1	30	1	356	0.67	2.18E+04	WZO2
17	A 62	47.18	–4.29	1, 13	37	20	302	Ph02		80.5	1	17	1, 2	23	0.12	6.78E+03	WZO2
18	A 71	85.00	4.49	1	41	11	2800	Ind	16	78.5	1	15	1	219	1.07	6.96E+04	WZO2
19	A 74	72.66	–17.15	4, 5, 6, 13	61	16	800	Ind	1, 2	415	1	26.5	1	239	1.61	5.95E+04	WZO3
20	A 75	101.86	8.75	1, 3	69	12	1421	Ph02		28	1	42	1	217	0.19	4.50E+03	WZO1
21	A 78	81.30	–14.91	1	7	1	1165	Ind	9, 10	53.5	1	25	3	303	0.30	1.18E+04	WZO2
22	A 86	118.79	8.24	1, 2	54	7	2186	Ph02		31.5	1	20		314	0.33	1.63E+04	WZO2
23	Ba 1	171.30	–25.81	2	63	12	2077	Ph02		19	1	35.5	1	936	0.19	5.28E+03	WZO1
24	CN 1-5	2.29	–9.48	1	51	12	1664	Ph02		3.5	1	18	1	275	0.03	1.54E+03	WZO1
25	DeHt 2	27.65	16.92	2	32	4	2380	Ind	12	47	1	20		703	0.54	2.66E+04	WZO1
26	DeHt 4	48.76	–1.53	1, 2	64	9	6284	Ph02		20	1	20		168	0.61	2.98E+04	WZO2
27	DHW 1-2	11.40	17.99	15	46	9	1883	Ph02		13.5	1	20		591	0.12	6.04E+03	WZO3
28	DHW 5	111.09	11.64	1, 3, 4, 5, 6	84	12	330	Ind	1	264	2	5	1	67	0.42	8.27E+04	WZO4
29	EGB 4	143.60	23.82	1, 2	45	14	611	Ph02		55.5	1	20		254	0.16	8.05E+03	WZO3
30	EGB 6	221.59	46.36	4, 5	84	2	525	Ind	1	360	1	38.5	1	425	0.92	2.33E+04	WZO2
31	EGB 9	209.43	9.50	16	83	5	343	Ph02		152.8	3	20		57	0.25	1.24E+04	WZO4
32	ESO 320-28	291.43	19.26	1	5	5	6000	Ind	15	16	1	20		2017	0.47	2.28E+04	WZO2
33	HaTr 1	299.49	–4.12	16, 17	30	10	5925	Ph02		36	1	20		426	1.03	5.06E+04	WZO2
34	HDW 1	124.06	10.72	1, 3	45	16	530	Ind	1	135	1	20		99	0.35	1.70E+04	WZO3
35	HDW 5	218.99	–10.78	1, 18, 19	72	19	1962	Ph02		47	1	20		369	0.45	2.19E+04	WZO3
36	HDW 6	192.53	7.22	1	70	14	2256	Ph02		38	1	20		284	0.42	2.03E+04	WZO4
37	He 2-428	49.41	2.48	1, 2, 19	49	4	950	Ind	1	4.8	1	15	4	41	0.02	1.44E+03	WZO2
38	HFG 1	136.38	5.55	4, 5, 13	47	2	409	Ph02		250	1	14	1	40	0.50	3.47E+04	WZO1
39	HW 4	149.50	–9.28	4, 5, 6	90	8	380	Ind	1, 12	270	1	20		62	0.50	2.44E+04	WZO3
40	IC 4593	25.33	40.84	2, 7, 20	43	3	1082	Ph02		6.5	1	12.3	1	771	0.03	2.73E+03	WZO1
41	IW 1	149.71	–3.40	4, 5, 6, 13	75	9	510	Ind	1, 12	390	1	8.50	1, 5	30	0.96	1.11E+05	WZO3
42	IW 2	107.73	7.81	4, 5, 6, 13	43	13	650	Ind	1	450	1	12	1	89	1.42	1.16E+05	WZO3
43	Jacoby 1	85.50	46.50	5, 21	75	2	1100	Ind	29	327	4	20		893	1.74	8.54E+04	WZO2
44	JaFu 2	353.52	–5.00	6	73	2	9100	Ind	24	2.5	5						WZO3
45	Jn 1	104.21	–29.64	1, 2	24	1	755	Ind	1, 19	160	1	15	1	413.9	0.621	4.05E+04	WZO3

Table 1. continued.

No.	PN	l	b	Ref.	IA	e	D (pc)	Method	Ref.	θ ($''$)	Ref.	$V_{\rm exp}$ (km s^{-1})	Ref.	Z (pc)	R (pc)	$T_{\rm dyn}$ (yrs)	WZO stage
46	K 1-27	286.88	–29.58	1	55	16	1200	Ind	1	23	1	20		619	0.13	6.55E+03	WZO2
47	K 1-28	270.17	24.84	1	86	17				27	1	20					WZO2
48	K 1-3	346.98	12.46	1			1596	Ph02		46	1	17	1	347	0.36	2.05E+04	
49	K 1-6	107.05	21.39	22	45	14	760	St	33	108	6	20		284	0.40	1.95E+04	WZO3
50	K 2-2	204.15	4.73	1, 2, 4	79	7	630	Ind	12	207.5	1	10	1	52	0.63	6.21E+04	WZO3
51	K 4-5	26.65	–1.58	2	80	12	11477	Ph02		2.8	1	20		317	0.16	7.63E+03	WZO3
52	KeWe 3	238.42	–1.87	16, 23, 24	55	12	686	Ph02		120	3	20		22	0.40	1.95E+04	WZO3
53	KeWe 5	348.94	4.61	23	86	4	8000	St	25	7.5	7	20		644	0.29	1.42E+04	WZO2
54	KFR 1	296.38	3.14	25	60	17				47.5	8						WZO3
55	Lo 10	328.20	1.41	1	75	9				6	1						WZO2
56	LoTr 1	228.21	–22.14	4, 26	89	11	1500	St	30	66	1	20		580	0.48	2.35E+04	WZO3
57	M 1-46	16.45	–1.98	27			1300	Ind	5	5.5	1	7	1	45	0.03	4.85E+03	WZO1
58	M 2-2	147.87	4.20	1, 2	74	8	1595	Ph02		3.05	1	14.3	1	117	0.02	1.61E+03	WZO2
59	M 2-40	24.12	3.88	1, 2, 28, 29	53	5	2016	Ph02		2.5	1	18	6	137	0.02	1.33E+03	WZO1
60	M 2-44	28.60	1.66	1, 2	50	13	1520	Ph02		3.7	1	12	1	44	0.03	2.22E+03	WZO1
61	MA 3	23.02	4.31	28, 30	35	17				2.5	1	5	6				WZO1
62	MeWe 1-1	272.41	–5.97	16, 17, 24, 25	80	2	1170	Ind	18	55	1	20		122	0.31	1.53E+04	WZO3
63	MeWe 1-2	283.45	–1.39	16, 24	61	10				132	9						WZO4
64	MeWe 1-4	315.99	8.24	16, 17, 24	75	9	2170	Ph02		65.25	3	20		312	0.69	3.36E+04	WZO3
65	MeWe 2-4	314.09	10.68	16, 24	56	14				240	8						WZO3
66	MWP 1	80.36	–10.41	5	68	7	600	Ind	1	5.5	10	20		109	0.02	7.83E+02	WZO3
67	NeVe 3-1	275.89	–1.02	16, 23, 24	47	5				28.75	8						WZO3
68	NeVe 3-6	292.48	0.88	31	70	4	5000	Ind	20	19.75	8	20		77	0.48	2.34E+04	WZO3
69	NGC 1360	220.36	–53.93	1, 35	50	15	385	Ind	1, 3	192.5	1	28	1	362	0.36	1.26E+04	WZO2
70	NGC 2438	231.80	4.12	14, 23	63	9	2000	Ind	7	32	1	21.2	1	144	0.31	1.43E+04	WZO1
71	NGC 2440	234.84	2.42	23, 33	49	5	1753	Ind	21	8	1	22.5	1	74	0.07	2.96E+03	WZO1
72	NGC 246	118.86	–74.71	1, 4, 33, 34	74	8	450	Ind	1	122.5	1	39.5	1, 2	587	0.27	6.62E+03	WZO3
73	NGC 2867	278.16	–5.94	1	49	10	1900	Ind	21	7	1	21.2	1	197	0.06	2.98E+03	WZO1
74	NGC 2899	277.15	–3.83	36, 37, 38	78	2	687	Ph02		45	1	25	1	46	0.15	5.87E+03	WZO2
75	NGC 3242	261.05	32.05	1, 32, 35	76	13	420	Ind	1	12.5	1	22.5	1	235	0.03	1.11E+03	WZO1
76	NGC 3587	148.49	57.05	39, 40	67	3	550	Ind	1	85	1	37.67	1, 7	548	0.23	5.89E+03	WZO1
77	NGC 40	120.02	9.87	1, 8, 29	90	3	800	Ind	3, 8	24	1	26.33	1, 2	138	0.09	3.46E+03	WZO2
78	NGC 6578	10.82	–1.83	1, 27	34	6	2000	Ind	22	4.25	1	19.2	1	64	0.04	2.10E+03	WZO1
79	NGC 6629	9.41	–5.05	1, 27, 32, 33	53	4	1950	Ind	21	7.75	1	20.17	1, 8	172	0.07	3.56E+03	WZO1
80	NGC 6751	29.23	–5.94	41, 42			1961	Ind	21	10.25	1	39	1	203	0.10	2.45E+03	WZO1
81	NGC 6765	62.46	9.56	1, 2	45	6	1521	Ph02		20	1	35	1	254	0.15	4.13E+03	WZO1
82	NGC 6772	33.16	–6.39	32	77	12	1260	Ind	21	32	1	17.6	1	140	0.20	1.09E+04	WZO1
83	NGC 6781	41.84	–2.99	3	76	2	1567	Ind	21	54	1	18	1, 8	82	0.41	2.23E+04	WZO2
84	NGC 6804	45.75	–4.59	28	82	3	1525	Ind	21	17.5	1	24	1	122	0.13	5.28E+03	WZO1
85	NGC 6826	83.56	12.79	37, 38	45	4	1550	Ind	5, 8	12.5	1	11	1	346	0.09	8.36E+03	WZO1
86	NGC 6842	65.91	0.60	1, 3	85	3	2700	Ind	16	28.5	1	35	1	28	0.37	1.04E+04	WZO1
87	NGC 6853	60.84	–3.70	2, 4, 5	74	4	408	Ind	2, 11, 14	201	1	25.5	1	26	0.40	1.53E+04	WZO1
88	NGC 6891	54.20	–12.11	2	45	3	2800	Ind	5, 8	7.5	1	8.4	1, 8	592	0.10	1.19E+04	WZO1
89	NGC 6894	69.48	–2.62	1, 43			1000	Ind	16	20	1	43	1	46	0.10	2.21E+03	WZO1
90	NGC 7094	66.78	–28.20	1	57	3	1623	Ind	10, 12	47	1	45	1	799	0.37	8.05E+03	WZO2

Table 1. continued.

No.	PN	l	b	Ref.	IA	e	D (pc)	Method	Ref.	θ ($''$)	Ref.	V_{exp} (km s^{-1})	Ref.	Z (pc)	R (pc)	T_{dyn} (yrs)	WZO stage
91	NGC 7293	36.16	–57.12	1, 4, 5	45	2	218	Ind	2, 14	490	1	31	3	217	0.52	1.63E+04	WZO1
92	Pe 1-16	26.34	–2.28	1	62	9	6156	Ph02		3.8	1	20		245	0.11	5.55E+03	WZO2
93	PFP 1	222.13	3.91	44	10	4	334	Ph02		570	11	20		23	0.92	4.51E+04	WZO2
94	PG 1034+001	247.55	47.75	10	79	11	155	St	34	10800	12	20		129	8.12	3.97E+05	WZO4
95	PM 1-295	51.36	1.81	28	5	17	1700	St	27	10	1	17	6	54	0.08	4.75E+03	WZO1
96	PN in M 22	9.87	–7.56	4	57	5	2700	Ind	31, 32	4.25	1	20		356	0.06	2.72E+03	WZO3
97	PW 1	158.92	17.86	4, 5	76	8	333	Ind	1, 2	600	1	24.7	1, 2	104	0.97	3.84E+04	WZO2
98	RE 1738+665	96.89	31.96	5	76	13	190	Ind	1, 2	1800	13	20		106	1.66	8.12E+04	WZO4
99	S 174	120.22	18.43	5	52	15	540	Ind	1, 12	375	13	20		174	0.98	4.81E+04	WZO3
100	S 176	120.29	–5.40	4, 5, 13	82	4	630	Ind	1	360	1	19	1	59	1.10	5.67E+04	WZO3
101	S 188	128.05	–4.07	1, 2, 4, 5, 6, 13	47	8	650	Ind	1	170	1	40	1	46	0.54	1.31E+04	WZO3
102	S 200	138.13	4.12	4	25	9	580	St	26	170	14	13	1	42	0.48	3.60E+04	WZO1
103	S 216	158.49	0.47	4, 5, 33	62	5	130	Ind	1, 2	3000	13	7	5	1	1.89	2.64E+05	WZO3
104	S 68	30.67	6.28	5, 13, 33	75	14	700	Ind	1	200	1	6.6	9	77	0.68	1.01E+05	WZO4
105	S 78	46.83	3.84	5	84	17	1420	Ind	19	300	1	20		95	2.07	1.01E+05	WZO4
106	Sd 1	78.93	0.76	1, 2	16	3	1949	Ph02		3.8	1	20		26	0.04	1.76E+03	WZO2
107	Sn 1	13.32	32.74	3	57	9	11900	Ind	5	3	1						WZO3
108	SuWt 1	309.30	1.39	16	87	12	526	Ph02		34	1	20		13	0.09	4.25E+03	WZO3
109	Tc 1	345.24	–8.84	1, 16	87	15	2300	Ind	8	4.5	1	8	1, 2	355	0.05	6.14E+03	WZO1
110	Ton 320	191.40	33.08	5	39	6	350	Ind	1	900	13	20	1	202	1.53	7.48E+04	WZO3
111	Vy 2-3	107.60	–13.32	28	64	13	5185	Ph02		2.1	1	13.1	6	1206	0.05	3.95E+03	WZO1
112	WDHS 1	197.41	–6.44	4, 5	30	5	750	Ind	1	462.5	1	17	1, 5	84	1.68	9.69E+04	WZO3
113	We 1-5	216.31	–4.49	1	61	6	5716	Ph02		7.5	1	20		448	0.21	1.02E+04	WZO2
114	We 1-6	224.94	1.06	1	2	9	1100	Ind	13	31	1	20		20	0.17	8.09E+03	WZO2
115	WeSb 5	58.69	–5.58	3, 24	80	5	1200	St	28	75	1	20		117	0.44	2.14E+04	WZO3
116	Wray 17-18	262.65	–4.62	1	30	8	6846	Ph02		10	1	20		552	0.33	1.62E+04	WZO2
117	YM 16	38.71	1.97	6	56	6	500	St	17	152	1	20		17	0.37	1.80E+04	WZO3

Notes. References for interaction: (1) Soker (1997); (2) Wareing et al. (2007); (3) Rauch & Kerber (2005); (4) Borkowski et al. (1990); (5) Tweedy & Kwitter (1996); (6) Dgani & Soker (1998); (7) Soker (1999); (8) Ramos-Larios et al. (2011); (9) Tweedy & Kwitter (1994a); (10) Rauch et al. (2004); (11) Jacoby (1981); (12) Kwitter et al. (1988); (13) Xilouris et al. (1996); (14) Pierce et al. (2004); (15) Kerber et al. (1997); (16) Kerber et al. (2000a); (17) Kerber (1998); (18) Ali & Pfleiderer (1999); (19) Soker & Hadar (2002); Zucker & Soker (1993); (21) Jacoby & Van de Steene (1995); (22) Frew et al. (2011); (23) Kerber et al. (1998); (24) Ali et al. (2000); (25) Rauch et al. (2000); (26) Bond & Livio (1990); (27) Corradi et al. (2003); (28) Guerrero et al. (1998); (29) Martin et al. (2002); (30) Villaver et al. (2003); (31) Kerber et al. (2000b); (32) Ramos-Larios & Phillips (2009); (33) Wareing (2010); (34) Muthu et al. (2000); (35) Rauch (1999); (36) Corradi & Schwarz (1995); (37) Weinberger & Aryal (2004); (38) Aryal et al. (2009); (39) Guerrero et al. (2003); (40) Borkowski (1993); (41) Clark et al. (2010); (42) Chu et al. (1991); (43) Soker & Zucker (1997); (44) Tweedy & Kwitter (1994b); (45) Tweedy & Napiwotzki (1994); (46) Tweedy et al. (1995).
References for IPNe distance: (1) Pottasch (1996); (2) Harris et al. (2007); (3) Pottasch & Acker (1998); (4) Acker et al. (1998); (5) Zhang (1993); (6) Sabbadin (1986); (7) Pottasch (1983); (8) Cazetta & Maciel (2001); Kaler & Feibelman (1985); (10) Kaler et al. (1985); (11) Napiwotzki (2001); (12) Napiwotzki (1999); (13) Saurer (1995); (14) Benedict et al. (2009); (15) Rauch et al. (1996); (16) Giammanco et al. (2011); (17) Cahn & Kaler (1971); (18) Ali & Basurah (2008); (19) Napiwotzki & Schonberner (1995); (20) Ali (2006); (21) Bensby & Lundstrom (2001); (22) Mellema (2004); (23) Gathier et al. (1986); (24) Jacoby et al. (1997); (25) Kerber et al. (1998); (26) Hartl & Weinberger (1987); (27) Tajitsu & Tamura (1998); (28) Weinberger & Sabbadin (1981); (29) Werner et al. (1991); (30) Dengel et al. (1980); (31) Cudworth & Peterson (1988); (32) Cudworth (1990); (33) Frew et al. (2010); (34) Rauch et al. (2004).
* "Ind." means individual distance, "Ph02" means distances calculated according to Phillips distance scale (2002) and "St." means statistical distances from literature.
References for IPNe radius: (1) ESO-Strasburg Catalog; (2) Ishida & Weinberger (1987); (3) Kerber et al. (2000b); (4) Jacoby & Van de Steene (1995); (5) Jacoby et al. (1997); (6) Kohoutek (1962); (7) Kerber et al. (1998); (8) Kerber et al. (2000a); (9) Melmer & Weinberger (1990); (10) Vauclair et al. (1998); (11) Pierce et al. (2004); (12) Rauch et al. (2004); (13) Tweedy & Kwitter (1996); (14) Borkowski et al. (1990).
References for IPNe Expansion Velocity: (1) ESO-Strasburg Catalog; (2) Weinberger (1989); (3) Meaburn et al. (1998); (4) Rodríguez et al. (2001); (5) Pottasch (1996); (6) Guerrero et al. (1998); (7) Phillips (1984); (8) Sabbadin (1984); (9) Hippelein & Weinberger (1990).